American Journal of Engineering Research (AJER)
e-ISSN: 2320-0847 p-ISSN : 2320-0936
Volume-9, Issue-10, pp-89-97
www.ajer.org
Research Paper Open Access

Numerical Simulation of Submarine's Thermal Wake Flow Field under Multi Layered Models

Zhe-chao Yang,Kai-ye Hu, Shi Hu
College of Shipbuilding Engineering, Harbin Engineering University, Harbin, China
Corresponding Author: KaiyeHu

ABSTRACT: *Based on the analysis of the physical and hydrological characteristics of the world ocean thermocline and thermocline, the simplified physical model and numerical calculation model are established. The marine environment with stratified flow is simplified as continuous stratified flow with gradually changing temperature and linear distribution. The stratified flow with thermocline and extremely thin thermocline thickness can be regarded as strong stratified flow with abrupt temperature change in the upper and lower layers. The viscous CFD method based on RANS equation, VOF multiphase flow model and temperature density current model are used to simulate the steady motion of a simplified SUBOFF fairing boat under three different stratified flow modes. The thermal wake propagation and temperature attenuation ofsubmarine under different stratification modes are studied and analyzed. The results show that the mixing heat transfer between the thermal wake and the lower temperature seawater and the decay rate of the thermal wake temperature are different under different stratified flow models.*

KEYWORDS: *Submarine, stratified model, thermal wake, VOF method, temperature density current model*

Date of Submission: 06-10-2020 Date of acceptance: 19-10-2020

I. INTRODUCTION

Submarine has become an important military strategic weapon because of its rapid attack, sudden attack and concealment. With the improvement of noise reduction and noise reduction technology for submarines in recent years, non-acoustic submarine detection technology has gradually become the main research direction of various countries[1-4]， Among them, infrared submarine detection has a broad application prospect because of its good concealment, high precision, real-time imaging, all-weather work around the clock and so on[5-7] .

Therefore, much attention has been paid to the wake effect of moving submarine in stratified flow. Zhang Jian [8] The temperature characteristics of cooling water discharged from submarine under linear temperature and density stratified flow are numerically simulated. It is found that the temperature gradient has an obvious inhibition effect on the buoyancy of thermal wake.Chen Shengtao[9-10]studied the attenuation characteristics of the thermal wake temperature of submarine with propeller. The results show that the temperature attenuation of thermal wake near the propeller is oscillatory, and then decreases slowly; the thermal wake rises obviously in the initial stage of cooling water discharge, and then increases in density due to heat exchange with surrounding seawater, and the buoyancy is no longer obvious. In the subsequent research, Chen Shengtao[11] found through numerical simulation that the higher the speed of the submersible, the longer the thermal wake formed on the sea surface, the wider the diffusion range of the thermal wake, and the relative distance of the thermal floating point almost has a logarithmic relationship with the velocity. Wu Mengmeng[12] applied the VOF multiphase flow model to study the changes of surface temperature, density and other characteristic parameters at different times during the cooling water discharge process in two-dimensional temperature uniform and linear stratified flow fields, as well as the influence of submarine's diving depth and speed on the longitudinal distribution of free sea surface temperature. Chen Boyi[13] numerically simulated the thermal wake diffusion process of a three-dimensional submersible in a temperature uniform fluid and a continuous stratified fluid, and the effect of bubbles in the fluid on the sea surface temperature characteristics. The results show that in the fluid with uniform temperature, whether there are bubbles or not, there will be thermal characteristics on the sea surface, but the thermal characteristics in the flow field with

bubbles will be more significant; in the fluid with temperature stratification, whether there are bubbles or not, the sea surface is cold, and this cold characteristic is more obvious than that in uniform flow.

According to the national standard， The standard critical values of the intensity of mesocline and thermocline in shallow water are 0.10 kg/m4 and 0.2 $℃/m$.In summer, the intensity of thermocline in the Yellow Sea area is the strongest, and the thermocline intensity is greater than that of Qingdao 1.50 $℃/m$,The maximum temperature is 1.98 $℃/m$, and the intensity of the mesocline is greater than 0.50 kg/m^4. Its upper boundary depth is 12 m and its thickness is 10 m, which is basically the strongest area in China offshore [14-15].In this paper, based on the three-dimensional incompressible RANS equation and VOF method, the density stratification is realized by using the temperature density current model to simulate the steady motion of an ellipsoid in the stratified flow containing a density cline, and then the influence of the stratification mode on the submarine thermal wake is investigated.

II. NUMERICAL METHOD

The continuity equation, i.e. the law of conservation of mass, can be expressed by the fact that the increase of fluid mass per unit time and the net mass flowing into the microelement in the same time interval must be equal. The expression is shown in equation(1)：

$$\frac{\partial \rho}{\partial t} + \nabla \cdot (\rho \vec{u}) = 0 \tag{1}$$

The law of conservation of momentum is actually Newton's second law, which can be expressed as the increase rate of fluid momentum in the infinitesimal body equal to the sum of various forces acting on the infinitesimal element. The mathematical expression of momentum conservation equation in, and directions is shown in formula (2) (3) (4):

$$\frac{\partial \rho u}{\partial t} + \nabla \cdot (\rho u \vec{U}) = -\frac{\partial p}{\partial x} + \mu(\frac{\partial^2 u}{\partial x^2} + \frac{\partial^2 u}{\partial y^2} + \frac{\partial^2 u}{\partial z^2}) + F_x \tag{2}$$

$$\frac{\partial \rho v}{\partial t} + \nabla \cdot (\rho v \vec{U}) = -\frac{\partial p}{\partial y} + \mu(\frac{\partial^2 u}{\partial x^2} + \frac{\partial^2 u}{\partial y^2} + \frac{\partial^2 u}{\partial z^2}) + F_y \tag{3}$$

$$\frac{\partial \rho w}{\partial t} + \nabla \cdot (\rho w \vec{U}) = -\frac{\partial p}{\partial z} + \mu(\frac{\partial^2 u}{\partial x^2} + \frac{\partial^2 u}{\partial y^2} + \frac{\partial^2 u}{\partial z^2}) + F_z \tag{4}$$

Where μ is the dynamic viscosity coefficient,uv w is the velocity component on the three axes,$F_x F_y F_z$is the mass force component, p is fluid pressure.

The law of conservation of energy, namely the first law of thermodynamics, can be expressed by the fact that the increase rate of thermodynamic energy in the micro element body is equal to the sum of the net heat flow into the micro element and the work done by the volume force and the surface force on the micro element. Without considering the change of kinetic energy, the energy conservation equation with temperature T as variable is shown in equation (5):

$$\frac{\partial (\rho T)}{\partial t} + div(\rho \vec{u} T) = div(\frac{k}{c_p} gradT) + S_T \tag{5}$$

Where, $T$is the temperature, $C_p$is the specific heat capacity, $k$is the thermal conductivity of the fluid, $S_T$is the energy source term of the fluid.

III. MODELING

The simplified SUBOFF fairing hull model designed by DARPA of the U.S. Defense advanced technology research agency is selected as the object of simulation analysis, and a drain pipe is attached. The length of the SUBOFF is 4.3559m, the maximum radius is 0.254m, and the radius of the drain pipe is 0.0313m. the center line of the drain is 0.22m below the center line of the hull, and the horizontal distance from the head end of the hull is 3.84m. In the right-hand rectangular coordinate system, the negative direction of x-axis is the motion direction of the submersible, z-axis is vertical upward, and the origin is 1.5m below the free water surface, which is consistent with the X and Y coordinates of the center of the head end of the submersible. In this study, STAR-CCM+ is used as the CFD solver, and the cutting mesh model is used for the mesh generation of the whole computational domain, and the hexahedron mesh is selected as the mesh type. The boundary layer grid is generated before the core mesh is generated. The height and total thickness of the first layer of prism layer grid are calculated by determining y^+, and the volume control of grid is set in the places where the geometric model is complex and has abrupt changes. The surface mesh refinement of SUBOFF 3D model with drain is shown in Fig.1.

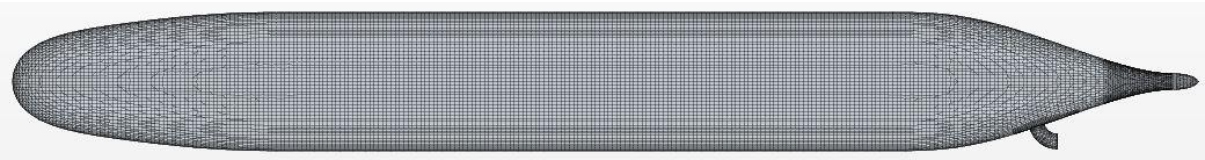

Fig. 1.Surface mesh refinement ofSUBOFF 3D model with drain

The free surface and wake region are separately encrypted by self-defined anisotropic mesh to capture the details of the thermal wake diffusion and buoyancy process and wake characteristics. The steady motion of submarine under water is simulated by inlet inflow. The boundary conditions are as follows: the inlet, top, bottom and side of the calculation domain are velocity inlet boundary conditions, the outlet is free outflow boundary condition, the submarine surface is static wall, the thermal condition is set as adiabatic, and the cooling water outlet is also set as velocity inlet boundary condition. The inlet and the side are treated with wave elimination. Fig. 2 shows the refined surface mesh of submarine model and the grid division diagram of layered flow calculation domain with thermocline. The calculation conditions are shown in Table 1.

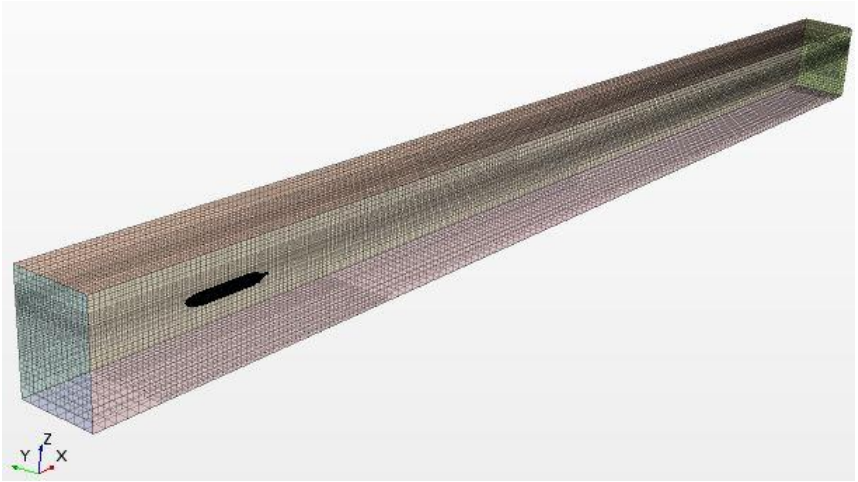

Fig. 2.Grid generation of hybrid stratified flow computing domain

Table 1 Calculation conditions of influencing factors of stratified mode

Case	Speed （m/s）	Depth （m）	Layered mode	Temperature （K）	Discharge rate （m/s）
1	0.7	1.5	Continuous	20	2
2	0.7	1.5	Thermocline	20	2
3	0.7	1.5	Strong	20	2

In the continuous linear stratified flow, the free surface temperature is set as *293.15K*, and the bottom temperature of the calculation domain is set as *291.15K*. The vertical temperature distribution function is shown in equation (6). Fig. 3 shows the vertical temperature distribution cloud of continuous stratified flow.

$$T = \begin{cases} 293.15 & z > 1.5\ m \\ 292.4 + 0.5 \times z & \text{-2.5} \le z \le 1.5\ m \end{cases} \quad (6)$$

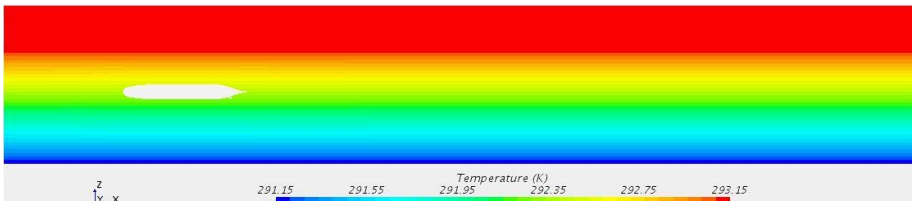

Fig. 3 Vertical temperature distribution nephogram of continuous stratified flow3

In the stratified flow with thermocline, the upper and lower bounds of thermocline correspond to$z=0.25m$ and$z=-0.25m$ respectively，The thickness of thermocline is $0.5m$,The thermocline intensity is $\Delta T/\Delta Z = 2K \cdot m^{-1}$,The temperature above the upper limit of the thermocline is set to $293.15K$，The temperature below the lower limit of the thermocline is set as $292.15K$，The temperature distribution in the middle of the thermocline is linear, and its vertical distribution function is shown in equation (7). Fig.5 shows the vertical temperature distribution nephogram of mixed stratified flow.

$$T = \begin{cases} 293.15 & z > 0.25\ m \\ 292.65 + 2 \times z & -0.25 \le z \le 0.25\ \text{m} \\ 292.15 & z < -0.25m \end{cases} \quad (7)$$

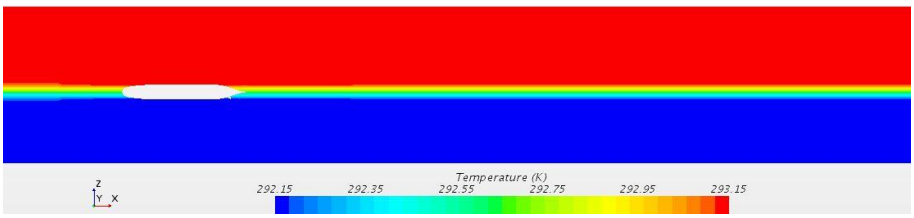

Fig. 5.Vertical temperature distribution nephogram of mixed stratified flow

The interface of strong stratified flow is located 2m below the free surface, corresponding to the vertical coordinate position of $z=-0.5m$. The temperature above and below the interface is set as $293.15K$ and $292.15K$ respectively. The vertical position distribution of temperature is defined by user-defined field function, as shown in equation (8). Fig. 6 shows the vertical temperature distribution of strong stratified flow.

$$T = \begin{cases} 293.15 z > -0.5m \\ 292.15 z \le -0.5\text{m} \end{cases} \quad (8)$$

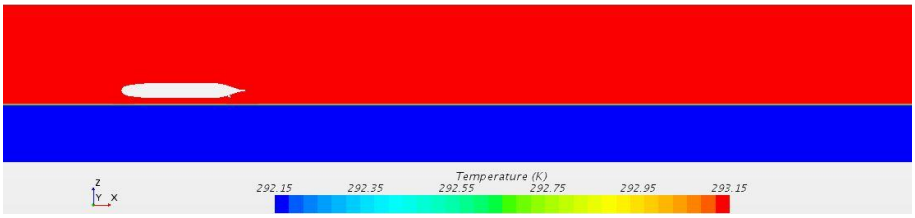

Fig. 6.Vertical temperature distribution nephogram of strong stratified flow

IV. NUMERICAL RESULTS AND DISCUSSION

According to the above model, $t = 100s$.The cloud chart of temperature distribution in longitudinal section of condition 1 is shown in Fig. 7, The cloud chart of temperature distribution at cross section $x=64m$is shown in Fig. 8, which shows that under the continuous stratification of temperature, the cooling water with higher temperature continuously exchanges heat with the surrounding seawater during the thermal wake diffusion process, and the temperature attenuation is serious. It can be seen from Fig. 8 that the temperature distribution of the thermal wake at$x=64m$tends to be circular. The higher the temperature is, the smaller the density is, which accelerates the vertical rise and diffusion of the thermal wake, so the diameter is slightly longer in the vertical direction than in the transverse direction.

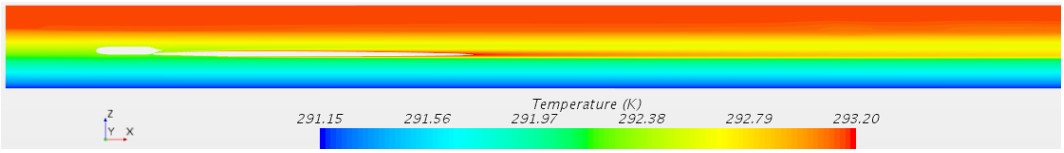

Fig. 7.Cloud chart of temperature distribution in middle and longitudinal section

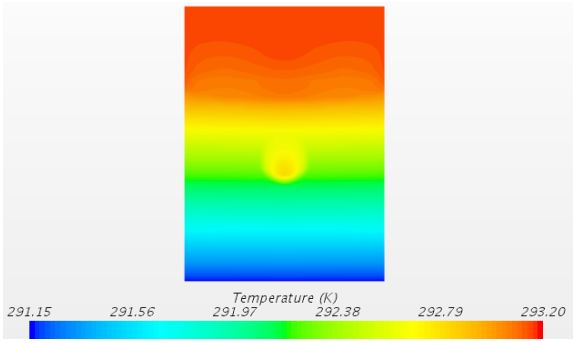

Fig. 8.Cloud chart of temperature distribution at x= 64m cross section

Fig. 9 shows the temperature distribution curve of the underwater vehicle's axis under different navigation time in condition 1. The central axis is a straight line along the direction passing through the coordinate, and the temperature of the background sea water at the central axis is *292.4K*. It can be seen from Fig. 9 that with the increase of time, the temperature value of thermal wake behind the submersible will tend to be stable; With the increase of the horizontal distance from the submarine, the temperature of the thermal wake increases first and then decreases, and then increases gradually in the vicinity. When t *=100s*, the maximum temperature is *292.925K*， at x *=13.375m*, and then decreases continuously. The temperature of the central axis at x *=64m* is about *292.704K*. Figure 10 shows the distribution curve of sea water center temperature with depth under different cross sections under condition 1 at t *=100s*. Due to the existence of continuous stratification and thermal wake, the central temperature of seawater first decreases and then increases with the increase of seawater depth, and finally drops to the same level as the background seawater temperature. In the future, with the increase of horizontal distance from the submarine, the maximum temperature in the center of sea water decreases, and the vertical distribution distance of temperature difference increases, which indicates that the temperature diffusion range gradually increases.

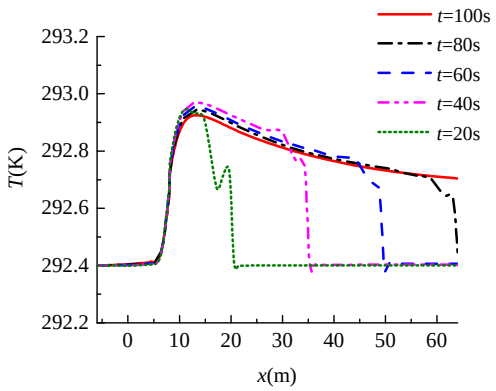

Figure. 9.Sea water temperature distribution along the axis of the submersible at different sailing times

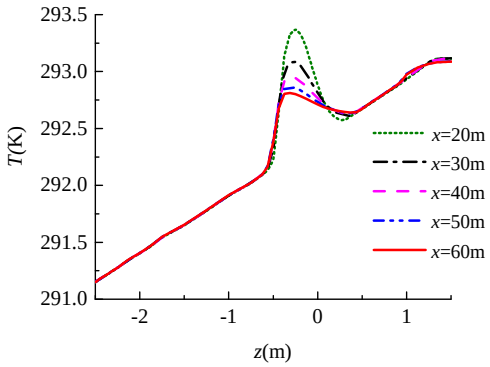

Fig. 10.Distribution of sea water center temperature with depth in different cross sections

The cloud chart of longitudinal section temperature distribution in case 2 is shown in Fig. 11, which shows that the temperature attenuation is serious in the process of thermal wake diffusion, and the diffusion range gradually increases and rises upward gradually. The mixed stratification of seawater temperature inhibits the rise of thermal wake. The color blank area of thermal wake temperature indicates that the longitudinal distance between the maximum temperature of seawater core greater than *293.2K* is *24.183m* from the cooling water outlet to the later.

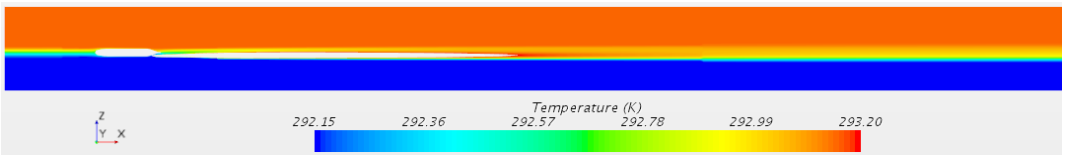

Fig. 11. cloud chart of temperature distribution in middle and longitudinal section

The temperature distribution nephogram of $x = 64m$ is shown in FIG. 12. The cloud image shows the mixing and stratification of seawater, and also shows that the temperature of the thermal wake gradually decreases after the diffusion heat transfer. It can be seen from Figure 12 that the temperature distribution of the thermal wake tends to be circular at $x = 64m$. The background sea water temperature is *292.65K* and the mixing and stratification of seawater temperature accelerate the diffusion and heat transfer of thermal wake.

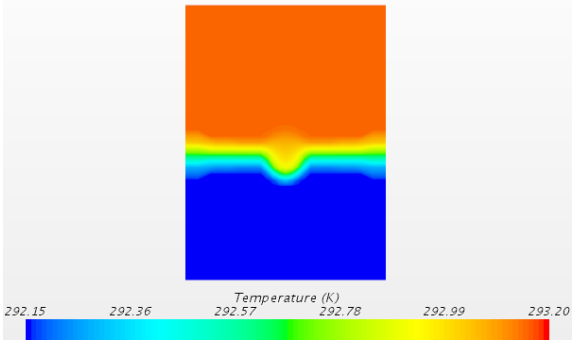

Fig. 12. temperature distribution nephogram of x = 64m cross section

Fig. 13 shows the temperature distribution curve of the central axis of the submersible under different sailing times. With the increase of time, the temperature of the thermal wake behind the submersible will tend to be stable; with the increase of the horizontal distance from the submarine, the temperature of the thermal wake first increases and then decreases, and then increases gradually near the submarine,When *t=100s*, the maximum temperature is *293.215 K* at *x=13.25m*, and then decreases continuously. The temperature of the central axis at *x=64m* is about *293.003K*.Fig. 14 shows the distribution curve of sea water central temperature with depth under different cross sections under condition 2 *T=100s*. Due to the existence of mixing stratification and thermal wake, the central temperature of seawater first decreases and then increases with the increase of seawater depth, and finally drops to the same level as the background seawater temperature. After *x=20m*, with the increase of the horizontal distance from the submarine, the maximum temperature in the center of the seawater decreases and the vertical distribution distance of the temperature difference increases, which indicates that the temperature diffusion range gradually increases.

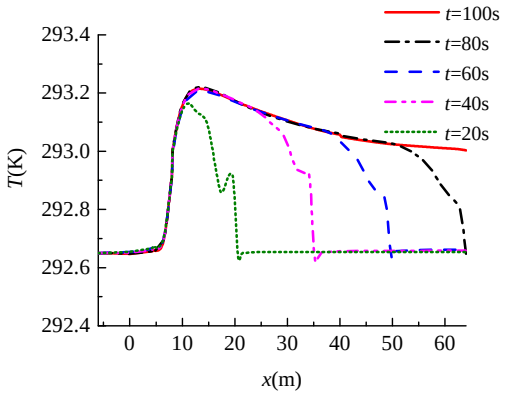

Fig. 13.Sea water temperature distribution along the axis of the submersible at different sailing times

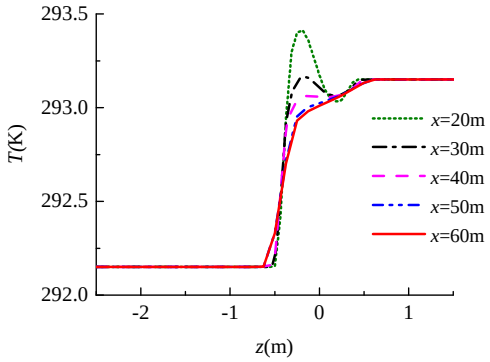

Fig. 14.Distribution of central temperature with depth in different cross sections

The cloud chart of temperature distribution in the middle and longitudinal section under condition 3 is shown in FIG. 15. In this condition, the submarine is located above the stratification interface, and the background seawater temperature of the central axis behind the submersible is *293.15K*, and the existence of strong stratification has no obvious inhibition on the buoyancy of thermal wake. Although the thermal wake temperature diffusion attenuation is serious, the temperature at the rear of the submarine at least 13.7 times the length is still greater than *293.2K*.

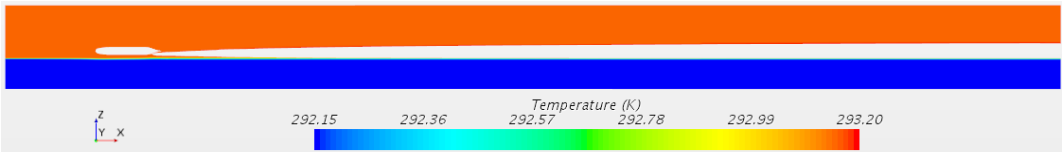

Fig. 15. cloud chart of temperature distribution in middle and longitudinal section

FIG. 16 shows the temperature distribution nephogram of *x=64m*. It can be seen from Figure 16 that the temperature distribution of the thermal wake tends to be trapezoidal at *x=64m*. Because the higher the temperature and the smaller the density, the vertical buoyancy and diffusion of the thermal wake will be accelerated. However, the lower temperature under the strong stratification of the seawater accelerates the diffusion and heat transfer of the thermal wake. Therefore, the length of the lower edge of the blank area in the figure is longer than that of the upper edge. The vertical height of the blank trapezoid area is about *0.9651m*, the upper edge coordinate *z=0.4917m*, the lower edge coordinate *z=⁻0.4734m*, ,and the horizontal length of the blank trapezoid section with *XOY* plane is *0.9396m*.

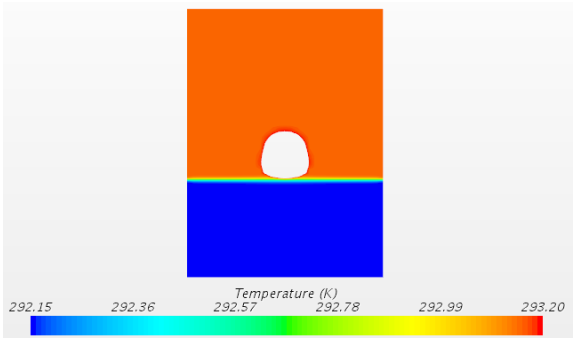

FIG. 16.Temperature distribution cloud of x = 64m cross section

Figure 16 shows the temperature distribution curve of the central axis behind the submersible under different sailing times in condition 3. It can be seen from Fig. 16 that with the increase of time, the temperature of thermal wake behind the submarine tends to be stable; with the increase of horizontal distance from the submarine, the temperature of thermal wake first increases and then decreases, and then gradually increases. When $t = 100s$, it reaches the maximum value at $x = 13m$, with the maximum temperature of $293.726K$, and then decreases continuously. The temperature of the central axis at $x = 64m$ is about $293.422K$. Figure 17 shows the distribution curve of the central temperature of seawater with depth under the cross section of condition 3 at $t = 100s$. Due to the existence of strong stratification and thermal wake, the central temperature of seawater first rises and then decreases with the increase of seawater depth, and then decreases to the same level as the background seawater temperature. After $x = 20m$, with the increase of horizontal distance from the submarine, the maximum temperature in the center of sea water decreases. The maximum temperature at $x = 60m$ is $293.58K$, and the vertical distribution distance of temperature difference is increasing, which indicates that the temperature diffusion range gradually increases.

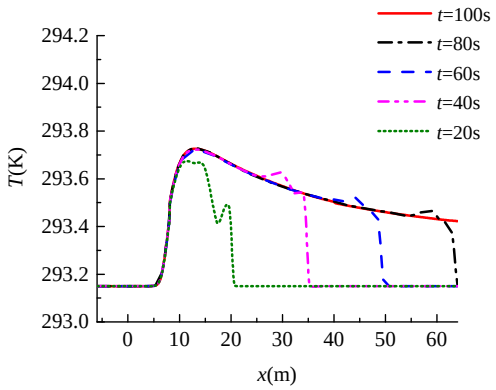

Figure. 16.Sea water temperature distribution along the axis of the submersible at different sailing times

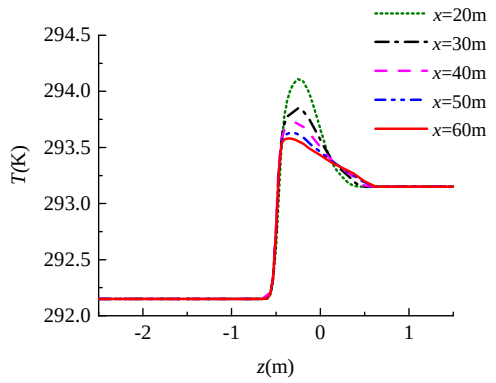

Figure. 17.Distribution of central temperature with depth in different cross sections

V. CONCLUSION

In this paper, the water body in the marine environment is simplified by stratification, and the mathematical models of continuous linear stratified flow, strong stratified flow and stratified flow with

thermocline are constructed. Taking the sub off fairing hull model with additional drainpipes as the research object, the combined working conditions of different stratification modes are divided, and the numerical simulation of the buoyancy and diffusion of the thermal wake of the submarine is carried out to explore the influence of the stratification mode on the thermal wake diffusion and temperature attenuation of the submarine.

(1) In the stratified flow with thermocline and continuous linear stratified flow, due to the non-uniformity of seawater temperature, the mixing heat transfer between the thermal wake and the lower temperature seawater is faster, which accelerates the temperature attenuation of the thermal wake. When the submarine is located above the strong stratified interface with the same temperature value of the surrounding seawater and the uniform flow, the temperature attenuation degree of the thermal wake has little change compared with that in the uniform flow.

(2) The buoyancy of thermal wake is related to the stratification of sea water and the relative position of submarine and thermocline. Generally speaking, when the submarine is in the thermocline of continuous stratification or mixed stratification, the stratification of seawater will inhibit the buoyancy of thermal wake, while when the submarine is in the strong stratified flow and above the interface, the stratification has no obvious inhibitory effect on the buoyancy of the thermal wake.

(3) The existence of moving submarine and thermal wake will disturb the stable stratification of sea water, which will cause the lower temperature seawater under the stratified flow to propagate upward and form a cold wake on the sea surface, especially in the continuous linear stratified flow.

REFERENCES

[1]. SHI Yu Jie, REN Haigang. Development trend of foreign non acoustic submarine detection and stealth technology [J]. Ship Electronic Engineering, 2015, 35 (1): 5-9

[2]. PENG Liang, WANG Jianxun, DENG Haihua, et al. Overview of underwater non acoustic detection and stealth technology [J]. Ship science and technology, 2014, 36 (5): 6-10

[3]. AI Yanhui, ZHAO Zhiping. Aspects of non acoustic detection technology [J]. Mine warfare and ship protection, 2003 (3): 43-46

[4]. CUI Guoheng, YU Dexin. Current situation of non acoustic submarine detection technology and countermeasures [J]. Fire and command control, 2007, 32 (12): 10-13.

[5]. YANG Haipeng, WANG Dan. Infrared detection of ocean internal waves [J]. Ship Electronic Engineering, 2012, 32 (10): 17-18 + 25.

[6]. WANG Jianhua, ZHAO Haosong. Overview of airborne infrared submarine detection system [J]. Laser and infrared, 2013, 43 (6): 599-603.

[7]. ZHAO Xianqi, YOU Yunxiang, CHEN Ke, et al. Experimental Study on the Generation of Internal Waves by a Slender Body in Stratified Fluid[J]. Journal of Shanghai Jiaotong University, 2009,43(08):1298-1301.

[8]. GUO Yan, WANG Jiang An, HE Yingzhou. Theoretical analysis of infrared thermal image water surface tracking detection [J]. Journal of Naval Engineering University, 2002, (03): 89-92 + 108.

[9]. CHEN S, ZHONG J, SUM P. Numerical Simulation and Experimental Study of the Submarine's Cold Wake Temperature Character[J]. Journal of Thermal Science, 2014, (03): 253-258.

[10]. WANG Jiang An, LIU Chaolong, JIANG Chuanfu. Study on buoyancy characteristics of submarine thermal jet [J]. Ship science and technology, 2006, (05): 15-18.

[11]. CHEN Shengtao, LIU Huanying, QI Yi. Study on mass transfer and heat transfer characteristics of submarine thermal wake in marine environment [C]. Outstanding academic papers of China Society of Shipbuilding Engineering, 2010.

[12]. CHEN Shengtao. Study on mass transfer and heat transfer characteristics of submarine thermal wake in marine environment [A]. 2010 outstanding academic papers of China Society of Shipbuilding Engineering [C]. 2011:6.

[13]. WU Mengmeng, CHEN Boyi, ZHANG Xiufeng, et al. Study on the variation of water surface characteristic parameters caused by underwater vehicles in temperature stratified ocean [J]. Infrared technology, 2010, 32 (04): 242-246.

[14]. ZHANG Haiwei, YOU Yunxiang, et al. Numerical simulation of wake of a moving sphere in a two-layer viscous fluid [J]. Journal of Shanghai Jiaotong University, 2007(02): 194-198.

[15]. LIU Jinfang, MAO Kexiu, ZHANG Xiaojuan, et al. The general distribution characteristics of pycnocline of China Sea[J]. Marine Forecasts, 2013, 06: 21-27.

[16]. ZHANG Mengning, LIU Jinfang, MAO Kexiu, LI Yan, et al. The General Distribution Characteristics of Thermocline of China Sea[J]. Marine Forecasts, 2006, 23(4): 51-58.

[17]. Menter, F.R. Two-Equation Eddy-Viscosity Turbulence Models for Engineering Applications[J]. AIAA Journal, 1994, 32(8), 1598–1605.

KaiyeHu. "Numerical Simulation of Submarine's Thermal Wake Flow Field under Multi Layered Models." *American Journal of Engineering Research (AJER),* vol. 9(10), 2020, pp. 89-97.